

## NEW CCD OBSERVATIONS AND THE FIRST PHOTOMETRIC STUDY OF THE CONTACT BINARY AP UMi

N. S. AWADALLA<sup>1</sup>, M. A. HANNA<sup>1,2</sup>, M. N. ISMAIL<sup>3</sup>, I. A. HASSAN<sup>3</sup>, AND M. A. ELKHAMISY<sup>1</sup>

<sup>1</sup>Dept. of Astronomy, Stellar Lab., National Research Institute of Astronomy and Geophysics, Helwan, Cairo, Egypt

<sup>2</sup>Head of the optical observations unit of the Kottamia Center of Scientific Excellence of Astronomy and Space Sciences (KCSE ASSC), Egypt; [magdyh.nriag06@yahoo.com](mailto:magdyh.nriag06@yahoo.com)

<sup>3</sup>Department of Astronomy, Faculty of Sciences of El Azhar University, Cairo, Egypt

Received October 12, 2015; accepted April 20, 2016

**Abstract:** We obtain the first complete CCD light curves (LCs) of the contact binary AP UMi in the VRI bands and analyzed them by means of the PHOEBE code. A spotted model is applied to treat the asymmetry in the LCs. The LC morphology clearly shows the O’Connell effect and the solution shows an influence of star spots on both components. Such effect of star spots is common between the RS CVn and W UMa chromospherically active stars. Based on the obtained solution of the LCs we investigate the evolutionary state of the components and conclude that the system is a pre-intermediate contact binary ( $f = 0.29$ ) with mass ratio  $q = 0.38$ , and it is an A-type W UMa system where the less massive secondary component is cooler than the more massive primary one.

**Key words:** stars: binaries: close — binaries: eclipsing: W UMa — stars: individual AP UMi

### 1. INTRODUCTION

Photometric and spectroscopic studies of eclipsing binaries (EBs) are important to determine their physical and geometrical properties. EBs in turn are important for testing stellar evolutionary models and can be used to determine mass and radius for both components of the binary system (e.g., Guinan et al. 2000; Torres & Ribas 2002).

One specific class of EBs is the W Ursae Majoris (W UMa) type systems whose light curves show continuous brightness variations and strongly curved maxima and minima with nearly equal depths. Binnendijk (1970) classified the W UMa binaries into two subclasses: A-type and W-type. The A-type binaries show moderate light curve variation (in comparison to W-type) or none at all and show deeper primary minima due to transit of the larger hotter component while the W-type binaries show primary minima due to occultation of the smaller less massive component. In general, orbital periods of A-type binaries are less than 0.3 day while for the W-type they are typically between 0.3 day and less than a day. In the case of W-type stars, which are contact or over-contact binaries, both components fill or over-fill their critical Roche lobes and are enclosed by a common convective envelope (e.g., El-Sadek 2012, and the references therein).

The evolution of the W-UMa type binaries has been discussed with more details in several studies (e.g., Vilhu 1982; Eggen & Iben 1989; Bradstreet & Guinan 1994). Most light curves of the W UMa binaries show the O’Connell effect, where a difference between the primary and secondary maxima is observed despite both components having nearly the same effective tempera-

tures (O’Connell 1951). This asymmetry in the light curve maxima is often associated with the presence of star spot(s) on one or both components which is quite important in understanding the light variations of the W UMa binaries.

We aim at following several newly discovered W UMa systems observationally in different bands, analyze the obtained light curves and obtain new minima times, to enlarge the data base of these interesting short period eclipsing binaries which usually represent contact binaries that exhibiting a fairly sharp lower limit to their observed orbital periods, of around 0.22 day (Rucinski 2007; Lohr et al. 2012).

We study the variability of the newly discovered faint eclipsing binary system GSC 4405-00129 (=USNOA2.0 1575-03371434 = USNOB1.0 1600-0101666 = ALLWISE J134253.35+700149.6) with  $V = 14.4 - 15.1$  (Khrusiov 2012), recently named AP UMi by Kazarovets et al. (2015). Khrusiov classified the system as an eclipsing W UMa type (EW) based on the light curve shape, as seen in Figure 1.

### 2. OBSERVATIONS

New observations in VRI standard Johnson filters for the faint EW-type binary AP UMi were carried out using an EEV CCD 42-40 camera attached to the Newtonian focus of the 74-inch reflector telescope of the Kottamia observatory in Egypt. The CCD camera has a format  $2048 \times 2048$  pixels with a scale of  $0''.308 \text{ pixel}^{-1}$  that was cooled by liquid nitrogen down to about  $-125^\circ\text{C}$ . The package C-Muniwin was used to reduce the CCD images.

We observed, in  $R$  and  $I$  bands, the variable (V), the comparison (C1) and the check (C2) stars during a very clear night of June 26, 2014. The identification

**Table 1**  
The coordinates of the variable (V) and comparison and check stars (C)

Star name	$\alpha_{2000}$	$\delta_{2000}$	mag <sub>V</sub>	mag <sub>B</sub>	mag <sub>R</sub>
V GSC 4405-00129 (AP UMi)	13 <sup>h</sup> 42 <sup>m</sup> 53 <sup>s</sup> .41 <sup>1</sup>	+70° 01' 49".56 <sup>1</sup>	14.69 <sup>2</sup>	15.12 <sup>2</sup>	14.23 <sup>3</sup>
C1 GSC 4405-00175	13 <sup>h</sup> 43 <sup>m</sup> 16 <sup>s</sup> .25 <sup>1</sup>	+70° 02' 18".56 <sup>1</sup>	–	16.83 <sup>3</sup>	14.73 <sup>3</sup>
C2 GSC 2.2 N11323326078	13 <sup>h</sup> 42 <sup>m</sup> 44 <sup>s</sup> .01 <sup>1</sup>	+70° 03' 04".05 <sup>1</sup>	–	14.93 <sup>3</sup>	14.23 <sup>3</sup>

<sup>1</sup> 2MASS Catalogue (Cutri 2003): yCat 22460C.

<sup>2</sup> NOMAD Catalogue (Zacharias et al. 2005), (2004): AAS 205, 4815.

<sup>3</sup> The USNO-A2.0 Catalogue. (Monet et al. 1998).

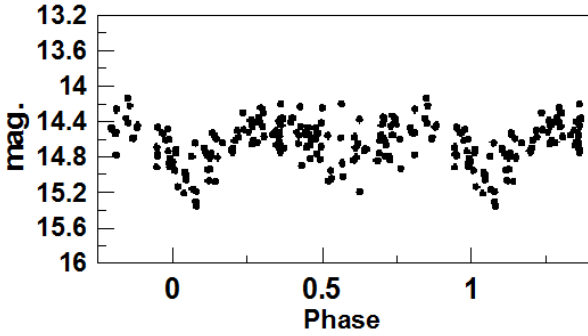


**Figure 1.** The light curve of the binary AP UMi without filter given by Khrusiov (2012).

field of the variable and comparison stars is shown in Figure 2. We used the following ephemeris given by Khrusiov (2012):

$$\text{HJD}(\text{Min.}) = 2\,451\,450^{\text{d}}.8120 + 0^{\text{d}}.25876 E, \quad (1)$$

The coordinates and magnitudes of the variable and comparison stars are listed in Table 1 according to the catalogues noted at the end of the table. We again observed the system in the *V*-band during a clear night of July 5, 2014. The exposure time taken in *V*, *R* and *I* filters were 230, 120 and 120 seconds, respectively. A total of 84 observations in *V*, 79 observations in *R* and 77 observations in *I* were obtained and listed in Table 7, where  $\Delta V$ ,  $\Delta R$  and  $\Delta I$  in the table denote the magnitude differences in the sense, variable minus comparison. Figure 3 represents the *V*, *R* and *I* LCs of the system AP UMi. The figure shows the differential magnitude versus the corresponding calculated phase obtained by our new ephemeris:

$$\text{HJD}(\text{Min.}) = 2\,456\,844^{\text{d}}.29461 + 0^{\text{d}}.2582867 E, \quad (2)$$

The new timings of one primary and one secondary minimum for each LC have been determined by using the paper tracing method. They are listed in Table 2.

In order to confirm that the comparison star C1 did not show any peculiar light variation, the magnitude differences between the comparison and check star  $\Delta \text{mag}$ . (C1-C2) for each filter are plotted on Figure 4, during the observational nights. They are linearly fitted giving standard deviations 0.012, 0.008 and 0.005 for *V*, *R* and *I* filter, respectively.

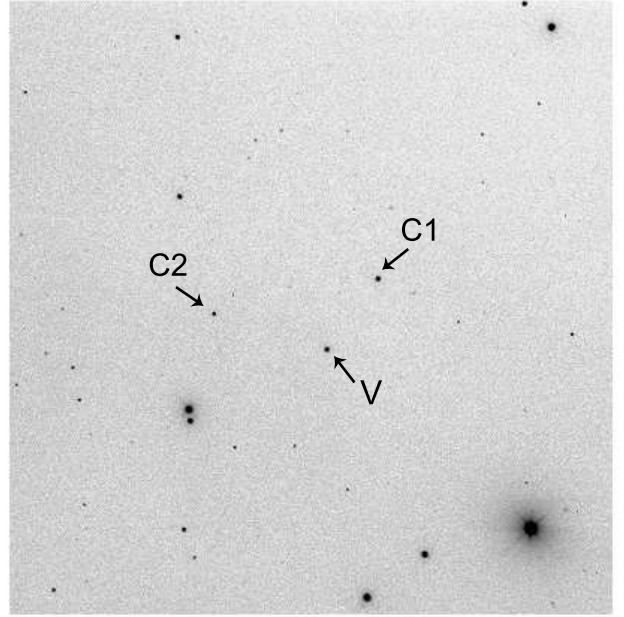


**Figure 2.** One of the CCD images of AP UMi (V), obtained using the 74 inch Telescope of the Kottamia observatory in Egypt. C1 and C2 are the comparison and check stars, respectively. North is up and east is to the left.

Also, the magnitudes of the comparison and check stars inside the atmosphere for Kottamia observatory, during the nights of observations, against the air mass were considered and plotted in Figure 5. Linear fits were applied and the results summarized in Table 3. From the values of the extinction coefficients given in Table 3, the atmospheric transparencies (*P*) have been calculated to be 73% and 74% (in the *V* filter) for the comparison and check stars, respectively. While for *R* and *I*, the transparency reached to 86% and 89-90% (Table 3), which indicate that the extinction coefficients in all filters were photometrically reasonable during all the nights of observations.

### 3. LIGHT CURVE ANALYSIS

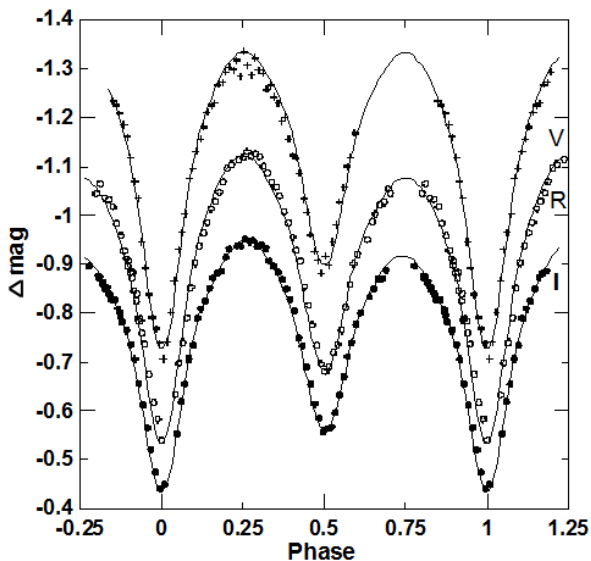
The observed light curves of AP UMi indicate typical short period W UMa eclipsing binary with narrow minima and broad maxima. To obtain the physical parameters of the system and to understand its geometrical structure, the new light curves were solved using the software PHOEBE (Prša & Zwitter 2005) and extensive

**Table 2**  
Times of minima (in days)

Min. time	Error	Filter	Type
2 400 000+			
56835.3659	0.0005	CCD R	II
56835.3664	0.0001	CCD I	II
56835.4971	0.0005	CCD R	I
56835.4972	0.0004	CCD I	I
56844.2946	0.0002	CCD V	I
56844.4201	0.0006	CCD V	II

**Table 3**  
Extinction coefficients

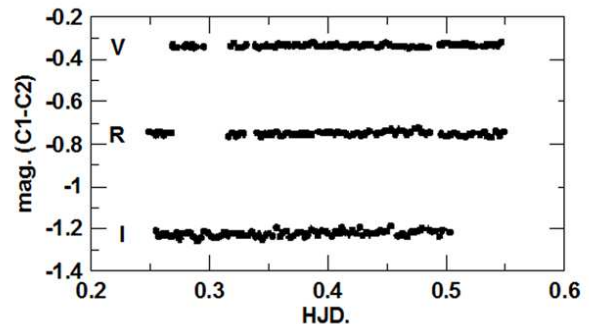
	Filter	Mag.-out	Ex. Coeff.	r	S.D.	P
C1	V	11.536	0.340	0.985	0.024	73%
	R	11.811	0.158	0.975	0.018	86%
	I	11.776	0.121	0.960	0.017	89%
C2	V	12.784	0.326	0.982	0.025	74%
	R	12.559	0.159	0.969	0.020	86%
	I	11.117	0.117	0.959	0.017	90%

**Figure 3.** The best match between the synthetic light curves and the observed light curves of binary AP UMi.

$q$ -search procedure. One of the facilities of PHOEBE program is that, we can analyze LC observed with different filters simultaneously. However, we observed the system AP UMi in R and I filters in one night, so we analyzed them simultaneously and the results are shown in Table 4; While the light curve of the V-filter was observed on another night, so we analyzed it separately and obtained nearly the same results as in case of R and I filters except  $l_1$  and  $l_2$  due to missing data in the secondary maximum and the presence of little scatter in the primary maximum.

We have applied a spotted model to treat the asymmetry in the LCs. and proceeded the solution by fixing the surface temperature of the primary star at 4500 K according to its spectral type K2.5 from Cox (2002, chapter 7, Table 6). Also, we used the “overcontact binary not in thermal contact” mode based on the general shape of the light curves.

Since no photometric solution for AP UMi was obtained till now, we first used a  $q$ -search procedure to determine the mass ratio. We searched for solutions with mass ratios from 0.1 to 0.68. The relation between the resulted sum  $\Sigma$  of the weight square deviation  $(O - C)^2$  and  $q$  is shown in Figure 6. The  $q$ -search of PHOEBE

**Figure 4.** Differential magnitude of comparison stars C1 and check star C2 as function of time.

converged and showed acceptable photometric solution for a contact configuration at about  $q_{ph} = 0.386$ . By using the van Hamme (1993) tables, the corresponding bolometric coefficients  $x_1 = -0.1599$  &  $x_2 = 0.74426$ , were interpolated. Following Lucy (1967) and Rucinski (1973) the gravity-darkening exponent  $g_1 = g_2 = 0.32$  and the bolometric albedo  $A_1 = A_2 = 0.5$  were assumed for both components with a convective envelope. With the assumed initial parameters, we continued the program process till the solution converged. Finally, we included the  $q_{ph}$  as an adjustable parameter and after some differential corrections the solution gave the final mass ratio of  $q_{ph} = 0.386 \pm 0.012$ . Solution parameters including standard errors of the obtained adjusted parameters are presented in Table 4. The theoretical light curves computed with these parameters are plotted in Figure 3 as solid lines. The fill-out factors for both components imply that AP UMi is a contact binary system.

## 4. DISCUSSION

### 4.1. Light Curves Morphology

In order to follow the light curve variation for the system, the light curve levels at maxima and minima have been measured directly from Figure 3. The magnitude difference between both maxima ( $D_{max.}$ ) and minima ( $D_{min.}$ ) and the depths of the primary ( $A_p$ ) and secondary ( $A_s$ ) minima for the observed light curves in the VRI bands are calculated using the following equations:

$$\begin{aligned}
 D_{max.} &= \text{mag}(\text{max.I} - \text{max.II}), \\
 D_{min.} &= \text{mag}(\text{min.I} - \text{min.II}), \\
 A_p &= \text{mag}(\text{min.I} - \text{max.I}), \\
 A_s &= \text{mag}(\text{min.II} - \text{max.I}),
 \end{aligned}$$

**Table 4**  
The light curve fit parameters by PHOEBE for AP UMi

Parameter	Filter V	Filter R and I	
$T_1$ (K)	4500	4500	
$T_2$ (K)	3865 ( $\pm 157$ )	3706 ( $\pm 92$ )	
Surface potential ( $\Omega$ )	2.604 ( $\pm 0.025$ )	2.583 ( $\pm 0.150$ )	
Mass ratio ( $q = M_2/M_1$ )	0.386 ( $\pm 0.012$ )	0.373 ( $\pm 0.01$ )	
Inclination ( $i$ )	81.3 ( $\pm 1.2$ )	77.5 ( $\pm 0.88$ )	
Albedo 1 ( $A_1$ )	0.5	0.5	
Albedo 2 ( $A_2$ )	0.5	0.5	
Gravity darkening Coeff. (g)	0.32	0.32	
Fill-out Factor $f$	0.285	0.293	
	Filter V	Filter R	Filter I
$l_1 = L_1/(L_1 + L_2)$	0.56	0.798 ( $\pm 0.024$ )	0.804 ( $\pm 0.022$ )
$l_2 = L_2/(L_1 + L_2)$	0.44	0.202 ( $\pm 0.017$ )	0.196 ( $\pm 0.017$ )
$x_1$	0.771 ( $\pm 0.12$ )	0.640 ( $\pm 0.011$ )	0.518 ( $\pm 0.015$ )
$x_2$	0.566	0.504	0.386

**Table 5**  
Magnitude differences and minima depths of AP UMi LCs.

Filter	$D_{max.}$	$D_{min.}$	$A_p$	$A_s$
V	–	0.175	0.628	–
R	–0.045	0.152	0.583	0.440
I	–0.030	0.125	0.509	0.393

**Table 6**  
Two spot parameters on the primary and secondary stars of AP UMi.

Parameters	Pri. star spot	Sec. star spot
Latitude ( $^\circ$ )	80	90
Longitude ( $^\circ$ )	110	110
Radius ( $^\circ$ )	9	5
Temp. Factor	0.2	1.55

and the results are listed in Table 5.

The morphological studies for the LCs (Figure 3) are as follows:

1. The primary minimum is deeper than the secondary in all filters (V, R and I). In the V filter the difference  $D_{min}$  is 0.175, in R 0.152, and in I 0.125 (i.e., the shorter the wavelength, the deeper the primary minimum).
2. The two maxima in the V-band are not exactly determined since no data was obtained in phase 0.75 but after fitting they appear to be the same. However, the magnitude differences (MaxI - MaxII) in the R- and I-bands are very clear and equal to –0.045 and –0.030, respectively (i.e., the O’Connell effect is clear for longer wavelengths).
3. The observed LCs indicate a typical partial eclipsing short period W UMA binary with broad maxima and narrow minima.

The obtained light curves fit parameters of the V, R, and I filters are listed in Table 4. From Table 4,

$T_1 > T_2$  (i.e., the primary minimum is deeper than the secondary one, see also Figure 3), the obtained mass ratio  $q$  is smaller than 0.54, and taking into consideration the Roche geometry configuration (Figure 7), one can deduce that AP UMi is likely to be an A-type W UMA system (see, Rucinski 1974).

The LCs analysis also shows two spots, cool spot on the primary component and a hot one on the secondary. The parameters of the two spots are given in Table 6, and the lobe configuration by PHOEBE is shown in Figure 8.

## 4.2. Color Indices Study

Pribulla et al. (2003) reported that the components of contact binaries are formed from almost normal, hydrogen-core-burning stars and the surface temperature of the contact binary depends on the orbital period. This so called period-color relation was first noticed by Eggen (1967) and empirically formulated by Wang (1994) as:

$$(B - V)_o = 0.062 - 1.31 \log P \quad (3)$$

where,  $(B-V)_o$  is the observed color index and  $P$  is the orbital period in days. For the contact binary AP UMi, the  $(B-V)_o$  value equals to 0.832. If we consider the well known equation of the color excess  $E(B-V)$  as follows:

$$(B - V)_i = (B - V)_o - E(B - V) \quad (4)$$

where  $(B - V)_i$  is the intrinsic color excess; and on applying the catalogued value of  $E(B-V) = 0.013$  from the All Sky Image Survey Catalogue, then we find that the spectral type for the system AP UMi is quite near K1.

To crosscheck this result we considered the magnitude values of J (=12.846), H (=12.319) and K (=12.177) from the 2MASS catalogue and calculated the color indices J-H, H-K and J-K. Also, the intrinsic color indices can be obtained by using the relative absorption values ( $A_\lambda$ ) from Schlafly & Finkbeiner (2011)

**Table 7**  
VRI-Observations of AP UMi

HJD(+2400000)	$\Delta V$	HJD(+2400000)	$\Delta R$	HJD(+2400000)	$\Delta I$
2456844.25442	-1.23419	2456835.25307	-0.75955	2456835.26870	-0.78181
2456844.25731	-1.22533	2456835.25461	-0.78764	2456835.27024	-0.79443
2456844.26020	-1.20836	2456835.25619	-0.78618	2456835.27181	-0.80868
2456844.26308	-1.18570	2456835.25776	-0.82395	2456835.27845	-0.83603
2456844.26601	-1.16056	2456835.25929	-0.84422	2456835.28000	-0.84208
2456844.26889	-1.11819	2456835.26085	-0.87152	2456835.28154	-0.84761
2456844.27178	-1.06842	2456835.26243	-0.88174	2456835.28315	-0.85441
2456844.27466	-1.03452	2456835.26398	-0.89649	2456835.28475	-0.86154
2456844.27756	-0.94622	2456835.26554	-0.91160	2456835.28628	-0.87404
2456844.28050	-0.89261	2456835.26713	-0.92703	2456835.28790	-0.87575
2456844.28346	-0.83782	2456835.31413	-1.04462	2456835.29476	-0.89610
2456844.28639	-0.79032	2456835.31583	-1.05355	2456835.31741	-0.88719
2456844.28927	-0.76765	2456835.31908	-1.02620	2456835.32066	-0.86947
2456844.29216	-0.73874	2456835.32237	-1.02258	2456835.32396	-0.86858
2456844.29508	-0.70633	2456835.32559	-1.00260	2456835.32717	-0.84998
2456844.29797	-0.74087	2456835.32881	-0.98691	2456835.33038	-0.83224
2456844.30099	-0.80225	2456835.33227	-0.94979	2456835.33811	-0.79934
2456844.30388	-0.86497	2456835.34006	-0.92011	2456835.34162	-0.77579
2456844.30677	-0.92947	2456835.34331	-0.90064	2456835.34487	-0.73933
2456844.30966	-0.96351	2456835.34649	-0.85750	2456835.34810	-0.71020
2456844.31256	-1.00342	2456835.34973	-0.81145	2456835.35131	-0.67034
2456844.31544	-1.07680	2456835.35301	-0.76459	2456835.35457	-0.63190
2456844.31832	-1.09484	2456835.35618	-0.73478	2456835.35779	-0.59569
2456844.32120	-1.12968	2456835.35940	-0.71791	2456835.36097	-0.56653
2456844.32409	-1.15609	2456835.36268	-0.69031	2456835.36427	-0.56323
2456844.32698	-1.18041	2456835.36588	-0.68133	2456835.36745	-0.55741
2456844.32987	-1.20985	2456835.36908	-0.69534	2456835.37065	-0.58372
2456844.33276	-1.22424	2456835.37280	-0.73360	2456835.37440	-0.61390
2456844.33565	-1.22890	2456835.37602	-0.77507	2456835.37759	-0.65447
2456844.33855	-1.26683	2456835.37928	-0.81589	2456835.38087	-0.68888
2456844.34156	-1.27110	2456835.38251	-0.85288	2456835.38409	-0.73231
2456844.34443	-1.29413	2456835.38571	-0.90611	2456835.38729	-0.74946
2456844.34733	-1.30317	2456835.38897	-0.92792	2456835.39054	-0.80521
2456844.35022	-1.29803	2456835.39216	-0.95517	2456835.39374	-0.82779
2456844.35326	-1.31706	2456835.39538	-0.98436	2456835.39694	-0.84883
2456844.35615	-1.28411	2456835.39857	-1.00708	2456835.40016	-0.86718
2456844.35908	-1.33422	2456835.40184	-1.03919	2456835.40341	-0.88320
2456844.36200	-1.30601	2456835.40531	-1.05860	2456835.40688	-0.89613
2456844.36492	-1.28668	2456835.40858	-1.06703	2456835.41015	-0.90610
2456844.36792	-1.32115	2456835.41177	-1.08567	2456835.41336	-0.93257
2456844.37091	-1.29613	2456835.41500	-1.10055	2456835.41658	-0.93852
2456844.37397	-1.29092	2456835.41831	-1.11913	2456835.41987	-0.93573
2456844.37704	-1.25698	2456835.42151	-1.12610	2456835.42310	-0.94747
2456844.37997	-1.26586	2456835.42473	-1.11932	2456835.42632	-0.94655
2456844.38289	-1.24111	2456835.42798	-1.12953	2456835.42957	-0.95032
2456844.38589	-1.22909	2456835.43119	-1.11720	2456835.43281	-0.93562
2456844.38878	-1.19132	2456835.43443	-1.11439	2456835.43600	-0.93658
2456844.39167	-1.20139	2456835.44057	-1.10420	2456835.44214	-0.93144
2456844.39456	-1.15705	2456835.44377	-1.09543	2456835.44534	-0.91349
2456844.39745	-1.12207	2456835.44696	-1.06874	2456835.44855	-0.88620
2456844.40032	-1.11654	2456835.45016	-1.04704	2456835.45173	-0.88036
2456844.40321	-1.08616	2456835.45334	-1.02739	2456835.45491	-0.87233
2456844.40610	-1.03263	2456835.45656	-1.01342	2456835.45813	-0.85035
2456844.40898	-1.00630	2456835.45984	-0.98447	2456835.46141	-0.82389
2456844.41186	-0.95972	2456835.46302	-0.96439	2456835.46459	-0.80873
2456844.41478	-0.92572	2456835.46621	-0.93640	2456835.46780	-0.78794
2456844.41768	-0.90790	2456835.46940	-0.90191	2456835.47098	-0.73368
2456844.42060	-0.88051	2456835.47269	-0.85170	2456835.47427	-0.70559
2456844.42356	-0.91585	2456835.47590	-0.78912	2456835.47748	-0.65458
2456844.42649	-0.89704	2456835.47917	-0.73948	2456835.48074	-0.61838

**Table 7**  
*Continued*

HJD(+2400000)	$\Delta V$	HJD(+2400000)	$\Delta R$	HJD(+2400000)	$\Delta I$
2456844.42937	-0.94497	2456835.48237	-0.69709	2456835.48394	-0.55284
2456844.43236	-0.98104	2456835.48556	-0.63271	2456835.49398	-0.44892
2456844.43526	-1.02668	2456835.49239	-0.50697	2456835.49720	-0.44177
2456844.43814	-1.05773	2456835.49563	-0.53920	2456835.50078	-0.47450
2456844.44107	-1.10010	2456835.49911	-0.58220	2456835.50429	-0.52096
2456844.44398	-1.11875	2456835.50260	-0.61569	2456835.50762	-0.56573
2456844.44692	-1.16750	2456835.50604	-0.67336	2456835.51088	-0.61199
2456844.44980	-1.18598	2456835.50931	-0.73708	2456835.51414	-0.65524
2456844.45280	-1.19850	2456835.51257	-0.78391	2456835.51735	-0.70458
2456844.45567	-1.26511	2456835.51576	-0.83992	2456835.52054	-0.73464
2456844.45856	-1.28527	2456835.51896	-0.88341	2456835.52375	-0.76424
2456844.46144	-1.28252	2456835.52218	-0.90666	2456835.53002	-0.80289
2456844.46436	-1.31609	2456835.52844	-0.95733	2456835.53321	-0.82665
2456844.46724	-1.32107	2456835.53164	-0.98291	2456835.53642	-0.82761
2456844.47014	-1.32364	2456835.53484	-1.01702	2456835.53978	-0.85203
2456844.47303	-1.32620	2456835.53821	-1.03247	2456835.54308	-0.86400
2456844.47609	-1.33001	2456835.54140	-1.03553	2456835.54631	-0.87289
2456844.47899	-1.34658	2456835.54473	-1.06402		
2456844.48480	-1.34571	2456835.54794	-1.04467		
2456844.48771	-1.36518				
2456844.49066	-1.36249				
2456844.49364	-1.36962				
2456844.49659	-1.35350				
2456844.50238	-1.31388				

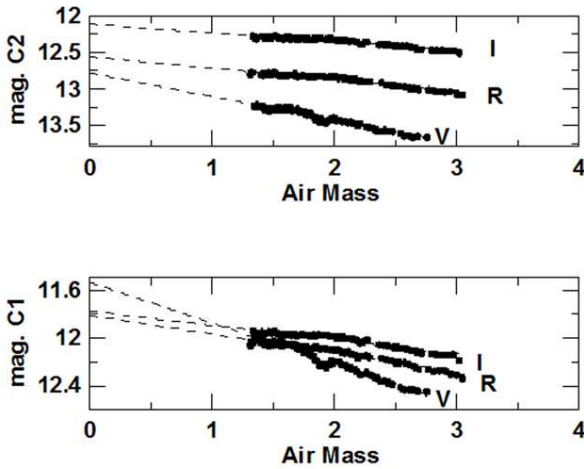


**Figure 5.** The relation between air mass vs the magnitude of C1 (lower panel) and C2 (upper panel) inside the atmosphere for different filters.

and Schlegel et al. (1998). Consequently we found nearly the same result that the spectral type of the primary is very close to K2. Of course this preliminary result should be confirmed spectroscopically.

## 5. CONCLUSIONS

1. The shape of the LCs (Figure 3) showed deep primary minima which classifies the system as an A-type W UMa system (Binnendijk 1970).
2. From the study of the color indices we can conclude

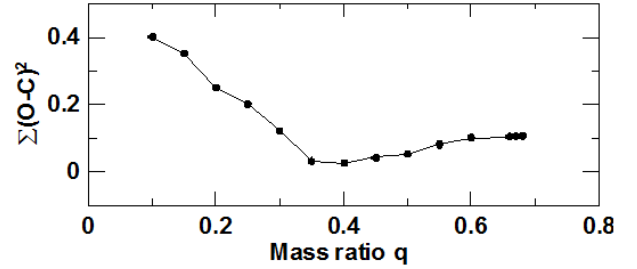


**Figure 6.** Relation between  $\Sigma$  and  $q$ .

that the system is of late spectral type (nearly K-type).

3. Even though the system was found to be of late spectral type, it is likely to be classified as A-type W UMa binary since it has  $T_1 > T_2$ , the mass ratio  $q < 0.54$  and its light curve shape appears to be of moderate activity (Smith 1984; Rucinski 1973, 1974).
4. The two spots have been found one cool spot on the primary with temperature factor 0.2, while the other spot on the secondary is hot with temperature factor 1.55 (Table 6).
5. The schematic picture of the Roche lobe (Figure 7) showed thin outer convective zone and common radiative envelope for both components which is a property of A-type W UMa systems (Rucinski 1974).

Spectroscopic observations for the binary system



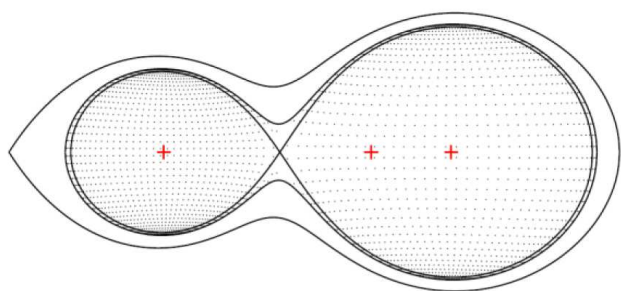


**Figure 7.** Roche lobe configuration of AP UMi.

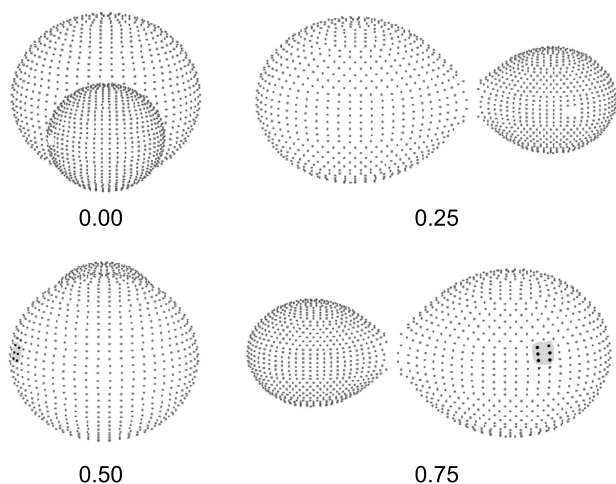


**Figure 8.** A schematic Spots modelling for AP UMi.

AP UMi are strongly recommended in order to determine its physical parameters to verify the obtained results.

#### REFERENCES

- Binnendijk, L. 1970, The Orbital Elements of W Ursae Majoris Systems, *Vistas in Astronomy*, 12, 217
- Bradstreet, D. H., & Guinan, E. F. 1994, Stellar Mergers and Acquisitions: The Formation and Evolution of W Ursae Majoris Binaries, in *ASP Conf. Ser.*, 56, 228
- Cox, A. N. 2002, *Allen's Astrophysical Quantities*, 4th edn. (New York: Springer)
- Cutri, R. M., Skrutskie, M. F., van Dyk, S., et al. 2003, *VizieR Online Data Catalog: 2MASS All-Sky Catalog of Point Sources*, yCat, 2246, 0
- El-Sadek, M. A. 2002, Study of the Properties of Some Late-Type Eclipsing Binary Systems, MSc Thesis, Cairo University, Egypt
- EGGEN, O. J. 1967, Contact Binaries II, *Mem. Royal Astron. Soc.*, 70, 111
- EGGEN, O. J., & Iben, I. J. 1989, Starbursts, Blue Stragglers, and Binary Stars in Local Superclusters and Groups. II – The Old Disk and Halo Populations, *AJ*, 97, 431
- Guinan, E. F., Ribas, I., Fitzpatrick, E. L., Gimenez, A., Jordi, C., McCook, G. P., & Popper, D. M. 2000, Eclipsing Binaries as Astrophysical Laboratories: Internal Structure, Core Convection, and Evolution of the B-Star Components of V380 Cygni, *ApJ*, 544, 409
- Kazarovets, E. V., Samus, N. N., Durlevich, O. V., Kireeva, N. N., & Pastukhova, E. N. 2015, The 81st Name-List of Variable Stars. Part I – RA 00h to 17h30, *IBVS* 6151
- Khrusiov, A. V. 2012, 43 New Variable Stars, *Peremennye Zvezdy Prilozhenie*, 12, No. 6
- Lohr, M. E., Norton, A. J., Kolb, U. C., Anderson, D. R., Faedi, F., & West, R. G. 2012, Period Decrease in Three SuperWASP Eclipsing Binary Candidates Near the Short-Period Limit, *A&A*, 542, 124
- Lucy, L. B. 1967, Gravity-Darkening for Stars with Convective Envelopes, *Z. Astrophys.*, 65, 89
- O'Connell, D. M. K. 1951, The So-Called Periastron Effect in Close Eclipsing Binaries; *New Variable Stars* (fifth list), Riverview Pub., 2, 85
- Monet, D. G. 1998, The 526,280,881 Objects In The USNO-A2.0 Catalog, *BAAS*, 30, 1427
- Pribulla, T., Kreiner, J. M., & Tremko, J. 2003, *Catalogue of the Field Contact Binary Stars*, CoSka, 33, 38
- Prša, A., & Zwitter, T. 2005, A Computational Guide to Physics of Eclipsing Binaries. I. Demonstrations and Perspectives, *ApJ*, 628, 426
- Rucinski, S. M. 1973, The Photometric Proximity Effects in Close Binary Systems. VI. The Exact Solution for the Source Function in Monodirectional Illumination of the Grey Atmosphere, *AcA*, 23, 301
- Rucinski, S. M. 1974, Binaries. II. A- and W-Type Systems. The W UMa-Type Systems as Contact, *AcA*, 24, 119
- Rucinski, S. M. 2007, The Short-Period End of the Contact Binary Period Distribution Based on the All-Sky Automated Survey, *MNRAS*, 382, 393
- Schlegel, D. J., Finkbeiner, D. P., & Davis, M. 1998, Maps of Dust Infrared Emission for Use in Estimation of Reddening and Cosmic Microwave Background Radiation Foregrounds, *ApJ*, 500, 525
- Schlafly, E. F., & Finkbeiner, D. P. 2011, Measuring Reddening with Sloan Digital Sky Survey Stellar Spectra and Recalibrating SFD, *ApJ*, 737, 103
- Smith, R. C. 1984, The Theory of Contact Binaries, *Quart. J. Royal Astron. Soc.*, 25, 405
- Torres, G., & Ribas, I. 2002, Absolute Dimensions of the M-Type Eclipsing Binary YY Geminorum (Castor C): A Challenge to Evolutionary Models in the Lower Main Sequence, *ApJ*, 567, 1140
- van Hamme, W. 1993, New Limb-Darkening Coefficients for Modeling Binary Star Light Curves, *AJ*, 106, 2096
- Vilhu, O. 1982, Detached to Contact Scenario for the Origin of W UMa Stars, *A&A*, 109, 17
- Wang, J. M. 1994, The Thermal Relaxation Oscillation States of Contact Binaries, *ApJ*, 434, 277
- Zacharias, N., Monet, D. G., Levine, S. E., Urban, S. E., Gaume, R., & Wycoff, G. L. 2004, The Naval Observatory Merged Astrometric Dataset (NOMAD), *AAS*, 205, 4815